## PAPER

Check for updates

# Degradable polymer films: RAFT-mediated emulsion copolymerization of lipoic acid with vinyl monomers

Steven W. Thompson, [ID] [a] Yasemin Fadil, [ID] [a] Nicholas J. Chan,[b] Graeme Moad, [ID] [b] Sébastien Perrier [ID] [c,d,e] and Per B. Zetterlund [ID] *[a]

The growing drive for sustainable materials has pushed the development of degradable polymers. This work explores the incorporation of α-lipoic acid (LA), a commercially available monomer capable of radical ring-opening polymerization (rROP), into polymer backbones using macroRAFT-mediated emulsion polymerization. A series of poly(butyl acrylate) (PBA) seed latexes with increasing LA content (up to 40 mol%) were synthesized and subsequently chain extended with *tert*-butyl acrylate (*t*BA) with up to 40 mol% LA and styrene (St) with up to 10 mol% LA to form diblock copolymers. Degradation studies revealed that thermolysis in DMF to cleave the C–S and S–S bonds was significantly more effective than using tris(2-carboxyethyl) phosphine (TCEP) to selectively target the S–S bonds. Substantial molecular weight reduction was observed from low LA mol% incorporation (<10 mol% LA), with minimal additional reduction with increasing mol% LA. Mechanical testing of PBA-*b*-PSt films demonstrated that at 5 mol% LA incorporation, minimal impact on mechanical properties was observed, while still enabling effective degradation. These findings highlight the potential of LA-based emulsion polymerization systems for producing scalable, degradable polymeric materials suitable for industrial applications such as coatings and adhesives.

### Green foundation

1. We developed an environmentally responsible approach using aqueous emulsion polymerization to prepare degradable polymers, polymer nanoparticles, and corresponding films. This method demonstrates the potential of water-based systems to deliver high-performance materials while maintaining a strong sustainability focus.

2. A key green chemistry achievement lies in the complete elimination of organic solvents, replacing them entirely with water as the polymerization medium. This not only minimizes hazardous emissions but also improves safety and reduces the environmental footprint of the process.

3. The method holds further potential for improvement by advancing room-temperature polymerization techniques, such as redox-initiated systems. By minimizing or even eliminating external heating requirements, the process could significantly reduce overall energy consumption, enhancing both its environmental credentials and economic feasibility.

## Introduction

Growing environmental concerns and the push for sustainable materials is a current major driving factor in the polymer science field.[1] One promising strategy to address this challenge is the incorporation of degradable comonomers into polymers, enabling controlled degradation while maintaining essential mechanical and functional properties.[2] Radical ring-opening polymerization (rROP) has emerged as a particularly attractive method for introducing degradable units into polymer backbones.[3] A key advantage of this approach is its compatibility with widely used vinyl monomers such as styrene (St), (meth)acrylates, and acrylamides.[4,5] Successful examples include the use of cyclic monomers such as cyclic ketene acetals (CKA),[6–8] macrocyclic allylic sulfides,[9–11] and dibenzo[c,e]oxepane-5-thione (DOT),[12–14] which introduce cleavable ester linkages. However, the practical application of these monomers is often limited by their complex and arduous synthesis, which poses challenges for large-scale implementation.

An emerging alternative cyclic monomer is α-lipoic acid (LA), a commercially available monomer that has recently

*[a]Cluster for Advanced Macromolecular Design (CAMD), School of Chemical Engineering, The University of New South Wales, Sydney, NSW 2052, Australia. E-mail: p.zetterlund@unsw.edu.au*
*[b]CSIRO Manufacturing, Bag 10, Clayton South, VIC 3169, Australia*
*[c]Department of Chemistry, University of Warwick, Coventry CV4 7AL, UK*
*[d]Warwick Medical School, University of Warwick, Coventry CV4 7AL, UK*
*[e]Faculty of Pharmacy and Pharmaceutical Sciences, Monash University, Parkville, VIC 3052, Australia*

gained significant attention. LA has a strained 1,2-dithiolane ring that undergoes rROP to introduce S–S and C–S linkages into polymer backbones.[15] LA and its derivates, such as ethyl lipoate, have been successfully incorporated by radical,[16,17] anionic[18] and cationic polymerizations.[19] In addition to copolymerization, LA and its derivatives have been employed as crosslinkers to synthesize degradable resins[20,21] and gels.[22] Albanese *et al.*[23] demonstrated that LA can be copolymerized with butyl acrylate (BA) using reversible addition–fragmentation chain transfer (RAFT) polymerization resulting in well controlled polymers with up to 30 mol% LA incorporation. Upon treatment with tris(2-carboxyethyl)phosphine (TCEP), a mild reducing agent, the S–S disulfide bonds were cleaved, resulting in a significant reduction in molecular weight (MW). Building on this work, the same group later reported[24] the conventional radical copolymerization of LA with St in solution. They also demonstrated that thermolysis at 100 °C in polar solvents such as dimethylformamide (DMF) could cleave C–S bonds, leading to enhanced degradation even for copolymers with low LA content. While much of the research to date has focused on solution polymerization, recent work by Morris *et al.*[25] extended this approach to miniemulsion polymerization, successfully incorporating LA with BA to produce stable, degradable latex particles. However, for broader industrial relevance, the development of degradable latex particles *via* emulsion polymerization remains a key goal in offering a more scalable and environmentally friendly route to degradable polymeric materials.

Emulsion polymerization is a vital industrial technique widely used for producing polymer latexes due to its ability to generate stable, high-solids-content dispersions with controlled particle size and morphology.[26,27] This process is often employed for the manufacture of coatings, adhesives, construction materials, and synthetic alternatives to natural products, offering a scalable and environmentally friendly route to functional polymers.[28] Among recent advancements, macroRAFT-mediated emulsion polymerization—also known as polymerization-induced self-assembly (PISA)—has emerged as a transformative approach.[29,30] This technique enables the one-pot synthesis of complex nanostructures[29,31,32] and multiblock copolymers[33,34] with high molecular weights and narrow molecular weight distributions (MWDs). It involves the *in situ* formation of amphiphilic block copolymers from water soluble macroRAFT agents, which undergo self-assembly into polymer particles.[35,36] Incorporating LA into RAFT emulsion systems presents a promising strategy for creating degradable, tailormade nanoparticles suitable for specialized industrial applications. While the incorporation of degradable cyclic monomers such as CKAs,[37] DOT,[38–40] and lipoate derivatives[41] has been explored, the use of LA in this context has not been reported.

In this work, P(BA-*stat*-LA) seed latexes are synthesized using macroRAFT-mediated emulsion polymerization using poly(methacrylic acid)-*b*-poly(methacrylic acid-*stat*-methyl methacrylate)-TTC (PMAA-*b*-P(MAA-*stat*-MMA)-TTC) with up to 40 mol% LA in the feed. From these seed latexes a series of chain extensions using *tert*-butyl acrylate (*t*BA) were performed with the same LA content in the feed as in the seed latexes. Degradation studies of both the seed latexes and diblock copolymers were conducted. Finally, a series of three PBA-*b*-PS diblock copolymers were synthesized with up to 10 mol% LA incorporation. These diblock copolymers were film formed directly from the latex with mechanical testing and degradation of the films explored.

# Results and discussion

## Seed latex synthesis

To synthesize stable emulsion copolymers containing LA, macroRAFT-mediated emulsion polymerization was chosen as it has been used for successful synthesis of stable, low dispersity seed latexes of common hydrophobic monomers such as PSt,[42–44] PBA[45,46] and poly(butyl methacrylate) (PBMA).[47–49] Previous work by Lages *et al.*[39] and Galanopoulo *et al.*[38] have used macroRAFT-mediated emulsion polymerization with DOT to generate degradable PBA and PSt seed latexes. In designing an industrially relevant emulsion system, care must be taken such that the mechanical properties are balanced with the film forming properties.[28,50] A feature of macroRAFT-mediated emulsion polymerization is that as the chains are to some extent "locked" in place as they are anchored at the particle surface *via* the hydrophilic segment,[46] the seed latex will form the outer layer of the particle and influence film forming properties heavily. Employing a low glass transition temperature ($T_g$) monomer such as BA is ideal then for designing an emulsion system to be able to undergo successful film formation.[46]

The initial focus was on the incorporation of LA into a PBA seed latex (degree of polymerization (DP) = 200) using macroRAFT-mediated emulsion polymerization. A PMAA$_{37}$-*b*-P (MAA$_4$-*stat*-MMA$_6$)-TTC macroRAFT agent was synthesized by a two-step, one pot solution polymerization (Scheme S2, detailed experimental conditions, $^1$H NMR and SEC data in the SI). As there is no purification step between the synthesis of the two blocks, the second block contains a small number of MAA units. The MAA units in the second block as well as only six units of MMA means that overall, the water solubility of the macroRAFT is still high. This type of macroRAFT has been shown to form hyper-coiled aggregates as opposed to micelles, meaning that the seed latex synthesis is a PISA process.[51] Our group has previously demonstrated that this type of macroRAFT agent can be successfully employed for synthesis of low dispersity, well-defined PS and PBMA seed latexes.[49,52,53] PBA seed latexes have previously been successfully synthesized with a purely hydrophilic PMAA-TTC macroRAFT, but the resultant particle size was larger than for similar systems using an amphiphilic macroRAFT.[46]

A PBA$_{201}$ seed latex without LA was first synthesized as a control (seed latex 1, Table 1) at 60 °C using VA-057 as the initiator at [RAFT]/[I] = 20.1 with a targeted solids content (SC) of 20%. Full conversion was reached within 1.5 h with a final particle size of 78 nm. The MWD was monomodal (Fig. 1) with

**Table 1** Experimental conditions and results for the synthesis of P(BA-*stat*-LA) seed latexes *via* macroRAFT-mediated emulsion polymerizations using PMAA$_{37}$-*b*-P(MAA$_4$-*stat*-MMA$_6$)-C12 (macroRAFT 1, Table S1) (see Table S2 for further details)

| Seed latex | Mol%$_{LA,th}$ | [M]/[RAFT] | [RAFT]/[I] | SC (%) | $X^a$ BA (%)/$t$ (h) | $M_{n,theo}^b$ | $M_{n,exp}^c$/$Đ$ | $Z_{av}$ (nm)/PDI$^d$ | Mol%$_{LA,exp}$ | $X$ LA$^e$ (%) |
|---|---|---|---|---|---|---|---|---|---|---|
| 1 | 0 | 201 | 20.1 | 20 | 99.5/3 | 31 800 | 29 250/1.68 | 78/0.09 | 0 | — |
| 2 | 5 | 200 | 20.0 | 20 | 100/6 | 32 450 | 29 000/1.63 | 78/0.02 | 4.3 | 86 |
| 3 | 10 | 200 | 20.3 | 20 | 100/6 | 33 250 | 28 750/1.63 | 75/0.09 | 8.9 | 88 |
| 4 | 20 | 200 | 20.3 | 20 | 99.0/6 | 33 800 | 27 900/1.72 | 75/0.07 | 18.6 | 91 |
| 5 | 30 | 200 | 20.2 | 20 | 94.1/6 | 36 400 | 27 050/1.70 | 74/0.04 | 29.2 | 91 |
| 6 | 40 | 200 | 20.1 | 20 | 98.0/6 | 37 950 | 28 000/2.06 | 74/0.08 | 37.7 | 89 |

$^a$ BA conversion/time determined by $^1$H NMR. $^b$ Theoretical $M_n$ calculated from eqn (S1). $^c$ $M_n$ and $Đ$ determined by SEC in THF calibrated with PS standards. $^d$ Z-Average diameter and PDI by DLS. $^e$ LA conversion calculated from $X$ BA and experimental mol% LA in copolymer.
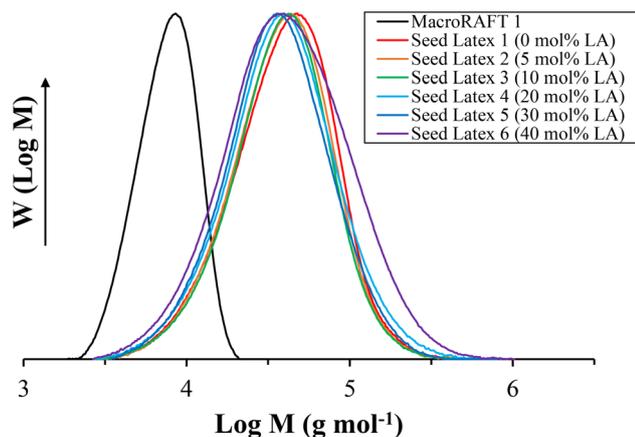


**Fig. 1** MWDs for P(BA-*stat*-LA) seed latex copolymers (seed latex 1–6, Table 1) synthesized *via* macroRAFT-mediated emulsion polymerizations using PMAA$_{37}$-*b*-P(MAA$_4$-*stat*-PMMA$_6$)-C12 (macroRAFT 1, Tables 1 and S1).



**Fig. 2** Conversion/time data of BA by $^1$H NMR for synthesis of P(BA-*stat*-LA) seed latexes (seed latex 1 and 5, Tables 1 and S1).

$M_{n,exp} \approx M_{n,th}$, however, the dispersity ($Đ$) was relatively high ($Đ$ = 1.68). Possible reasons for this are the lower SC (20%) compared with the previous PISA PMAA-TTC approach (SC = 34.2%).[46] The lower SC results in a lower concentration of macroRAFT hyper-coiled aggregates, which can reduce the overall control of the system. As this work is not focused on RAFT control, the higher $Đ$ is acceptable. A series of five P(BA-*stat*-LA) seed latexes (seed latex 2–6, Table 1) were subsequently synthesized with increasing theoretical LA content from 5 to 40 mol%. Previous work by Hawker and coworkers showed that LA has a limiting solubility in BA (9.6%).[25] However, as the polymerization temperature is 60 °C, similar to the melting temperature of LA, it will be a liquid during the polymerization. As a result, the limiting solubility should not be a factor in these polymerizations.

For all systems except seed latex 5 (30 mol% LA), >98% BA conversion was achieved in 6 h. Seed latex 5 had a lower BA conversion of 94.1%. All LA-containing systems required longer polymerization time to reach full conversion than seed latex 1 without LA and experienced a longer nucleation time. The kinetics of seed latex 1 and seed latex 5 show that the inclusion of LA into the seed latex increased the nucleation time from 30 min to 2 h (Fig. 2). For all polymerizations con-
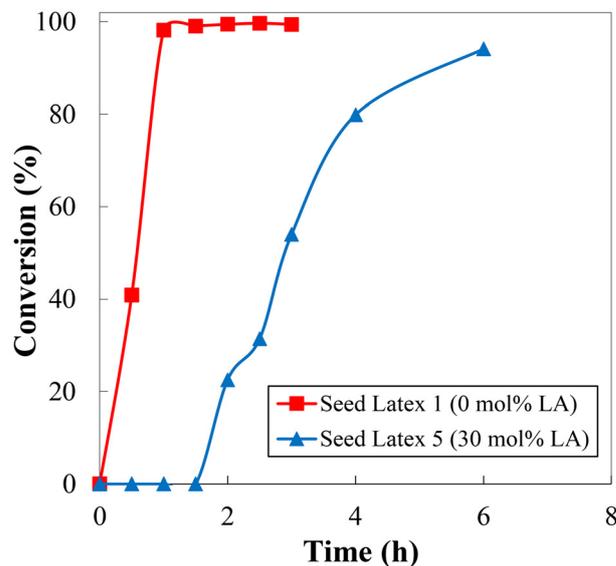
taining LA, the nucleation time was approximately constant at ~2 h as evaluated by visual observation of the onset of turbidity. The water solubility of LA has been shown to be limited[54] (0.003 M at 25 °C) and as such even at 5 mol%, the LA concentration in the aqueous phase has reached saturation. As a result, further increasing the mol% LA has no impact on nucleation time. It has been shown that LA is incorporated faster than BA in RAFT polymerization.[23] The longer nucleation time is attributed to slow propagation of LA monomer units during the initial growth of the hydrophobic segment of the macroRAFT. The polymerization rate after nucleation is also lower in the presence of LA. The ring size and substituent pattern have a large impact on the ring-opening of cyclic disulfides;[55] work by Zhang *et al.*[18] showed that when comparing LA to methyl asparagusic acid (another 1,2-diothiolane with a smaller substituent group), a 4.5 times decrease in polymerization rate was seen. Kinetic studies into copolymerization of DOT showed retardation in copolymerization with BA, which was attributed to slow fragmentation.[40] Overall, stable latexes with no coagulum were obtained for all seed latexes with par-

ticle size 74–78 nm and PDI < 0.1. The MWDs were monomodal for all seed latexes (Fig. 1), with similar $M_{n,exp}$ and $Đ$ for all systems except seed latex 6 (40 mol% LA), which had a slightly higher $Đ$ (2.08 compared to approx. 1.6–1.7). ^{1}H NMR (of methylated copolymer) analysis comparing the $CH_2$ peak from PBA (3.9–4.2 ppm) with the methyl peak on lipoate (3.6 ppm) (Fig. 3) revealed that LA was successfully incorporated into the polymer with increasing theoretical LA content up to 40 mol% LA. All the seed latexes showed slightly lower incorporation than the theoretical content (Table 1), with all seed latexes having an LA conversion of ~90%. Overall, the present data have demonstrated that using macroRAFT-mediated emulsion polymerization, P(BA-*stat*-LA) seed latexes can be synthesized with up to at least 37.7 mol% LA incorporation.

### Degradation of seed latexes

For the degradation of the seed latexes, two methods were employed. The first approach used TCEP, a mild reducing agent, in a 4 : 1 vol/vol THF/water solution at 60 °C.[23] 200 μl of latex was diluted in 1 ml of water and added to 4 ml of THF. The second approach involved dissolving 400 μl of latex in DMF (5 ml) and heating at 100 °C whilst open to air.[24] The TCEP approach selectively targets S–S disulfide bonds whereas

thermolysis in DMF targets both C–S bonds and S–S bonds. Okayama *et al.*[24] proposed that the degradation mechanism in polar solvents, such as DMF and NMP, takes place primarily by an oxidative mechanism which allows for the cleavage of both C–S bonds and S–S bonds. For degradation employing TCEP, almost no reduction in $M_n$ was seen with seed latex 2 and 3 (5 and 10 mol% LA) (Table 2 and Fig. 4). Seed latex 4 showed a slight reduction in $M_n$ from 27 900 g mol$^{-1}$ to 20 200 (Table 2 and Fig. 4) however, it is not until seed latex 6 (40 mol% LA) that a significant reduction in $M_n$ (Table 2) and clear shift in the MWD (Fig. 4) was observed. Given that the degradation only targets S–S disulfide bonds, it requires two units of LA to be next to each other along the polymer backbone, and such dyads would only be present in significant number at sufficiently high LA content. The macroRAFT agent does not contain any LA so will remain a significant component of the degraded polymer.

In contrast to the TCEP approach, thermolysis in DMF resulted in significant degradation for all seed latexes. Seed latex 2 degraded from 29 000 g mol$^{-1}$ to 2500 g mol$^{-1}$ (Table 2), with the MWD showing bimodality (Fig. 4), with the main peak overlapping with much of the macroRAFT peak and a smaller peak at a lower MW, indicating presence of small
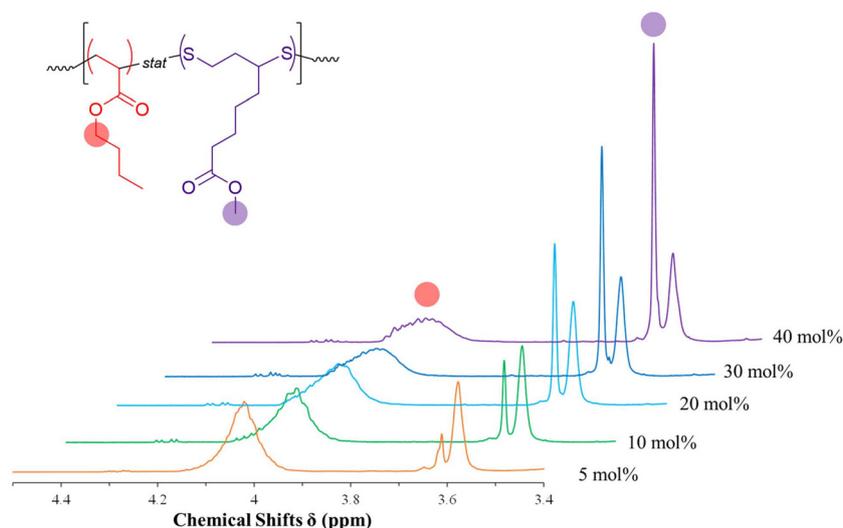


**Fig. 3** ^{1}H NMR spectra of methylated samples of P(BA-*stat*-LA) seed latexes (seed latex 2–6, Tables 1 and S1) with characteristic peaks highlighted. The mol% refer to initial mol% of LA in the monomer feed.

**Table 2** $M_{n,exp}$ and $Đ$ for seed latex 2–6 (Table 1) before degradation and after degradation *via* both the TCEP degradation approach and the DMF degradation approach

| Seed latex | 2 | 3 | 4 | 5 | 6 |
|---|---|---|---|---|---|
| Mol%$_{LA,th}$ | 5 | 10 | 20 | 30 | 40 |
| $M_{n,exp}$ (g mol$^{-1}$)/$Đ^a$ | | | | | |
| Seed latex | 29 000/1.63 | 28 750/1.63 | 27 900/1.72 | 27 050/1.70 | 28 000/2.06 |
| TCEP degradation | 28 050/1.67 | 28 100/1.66 | 20 200/1.84 | 16 850/1.69 | 9750/1.57 |
| DMF degradation | 2500/2.46 | 1750/2.20 | 700/2.51 | 550/1.98 | 500/2.09 |

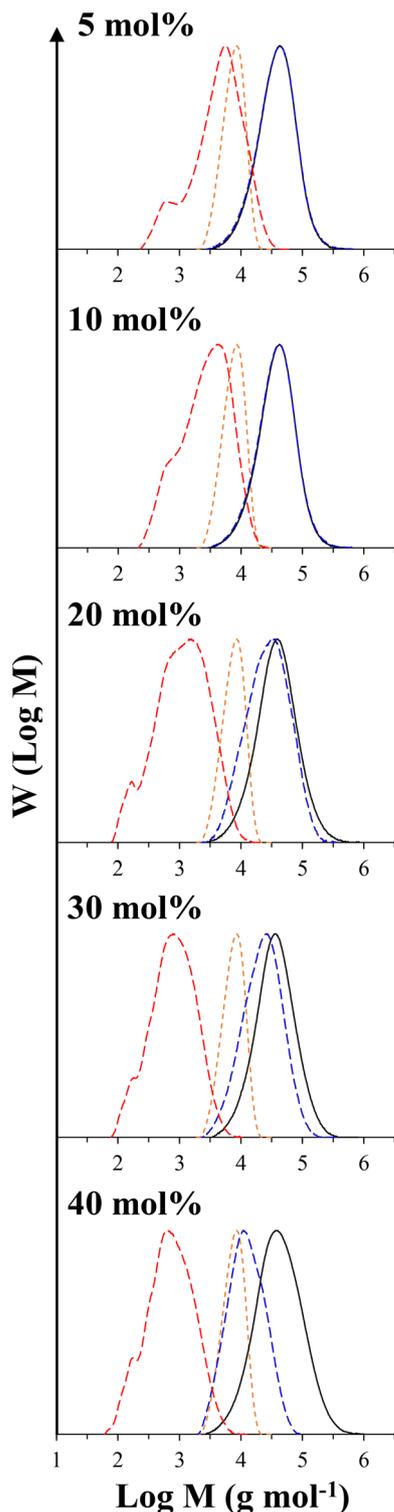$^a$ $M_n$ and $Đ$ determined by SEC in THF calibrated with PS standards.

**Fig. 4** MWDs for P(BA-*stat*-LA) seed latex copolymers (seed latex 2–6, Table 1) before (black trace) and after degradation *via* both the TCEP degradation approach (blue dotted trace) and the DMF degradation approach (red dotted trace) with macroRAFT MWD for visual comparison (orange dotted trace).

oligomers in the degraded product. Increasing the LA content resulted in further decrease in the MW, however, above 20 mol% LA, diminished gains in degradation were seen, only decreasing from 700 g mol$^{-1}$ for seed latex 4 to 500 g mol$^{-1}$ for seed latex 6. These results show that even with minimal LA content, significant degradation can occur and highlights that cleavage of C–S bonds is occurring in addition to S–S bonds. Okayama *et al.*[24] showed that for the degradation to occur *via* oxidative cleavage, the presence of oxygen in this system is vital and absence of oxygen can prevent degradation occurring.

It is possible to estimate the number of LA units incorporated per chain, thus enabling calculation of a theoretical minimum oligomer size after degradation. For the TCEP approach, it was assumed that all LA units are incorporated as dyads (adjacent monomer units; since only S–S bonds are severed). This analysis is made complex by the contribution of the macroRAFT, which does not degrade, and the RAFT end group which would be expected to be cleaved. Moreover, short oligomers may be below the limitations of the calibration of the SEC instrument and PS standards were used despite the degraded products containing oligomeric species of PBA and also PMMA segments from the methylated macroRAFT. In addition, the individual rates of monomer consumption are known to not be equal with LA incorporating preferentially over BA, although in theory this would not affect the calculation given it is concerned with number-averages.[23] Notwithstanding these shortcomings and complexities, this analysis does offer important insight into the extent of degradation in these systems.

For all polymerization using the TCEP approach (Table S5), the minimum theoretical value of $M_n$ after assumed complete degradation is much lower than the experimental (5950 compared to 28 050 g mol$^{-1}$ for seed latex 1 (5 mol% LA)). Even with high mol% LA as with seed latex 6, there is an order of magnitude difference between the theoretical (700 g mol$^{-1}$) and the experimental values (9750 g mol$^{-1}$). This is to be expected for a statistical copolymer, considering that the majority of LA units would not be incorporated as dyads. The theoretical $M_n$ after degradation was in very good agreement with the experimental $M_n$ for the DMF approach, suggesting that degradation is complete. The MWDs (Fig. 4) for the high mol% LA seed latexes showed only a small crossover where the macroRAFT peak would be expected, most likely due to the SEC calibration. PMMA standards were used for the macroRAFT, whereas PS standards were used for the degraded samples because the Mark–Houwink parameters for PBA are closer to PS compared to PMMA.[56,57] It is noteworthy that the lowest part of the MWDs extend to lower MWs than the original macroRAFT, which may initially seem odd given that the macroRAFT would not degrade as it does not contain LA. However, one must consider that the LA-containing polymer segments can degrade to segments shorter than the original macroRAFT.

**Chain extension of seed latex with *t*BA**

The next step was to chain extend the seed latexes to synthesize diblock copolymers. *t*BA was chosen as a different acry-

late monomer to explore the limits of the system. As with the seed latexes, the reaction temperature was 60 °C using VA-057 as the initiator but with a reduced [RAFT]/[I] ratio of 10. The targeted DP was 400 to explore the effect of LA on RAFT control for such a high target DP. Typically, in seeded RAFT emulsion polymerizations, lower block lengths improves RAFT control. The content of LA in the monomer feed of each chain extension corresponds to the amount of LA in the seed latex (*e.g.* chain extension 3 (10 mol% LA) was chain extended from seed latex 3 (10 mol% LA)).

For chain extension 1 (0 mol% LA), full *t*BA conversion was reached in 3 h, resulting in a stable emulsion with particle size 99 nm (Table 3). $M_{n,exp}$ was slightly lower than $M_{n,theo}$ with $Đ =$ 2.08. The MWD (Fig. S2A) was monomodal and shifting from the first block indicating successful chain extension. Chain extensions 2 and 3 (5 and 10 mol% LA) reached full *t*BA conversion within 6 h, resulting in stable latexes with no coagulum (Table 5). The $M_{n,exp}$ was much lower than $M_{n,theo}$ but the MWD (Fig. S2B and C) showed clear shifting from the seed latexes. Progressively from chain extension 4 onwards, the *t*BA conversion decreased from 95% for chain extension 4 to 40% for chain extension 6. Chain extension 6 had a large amount of yellow crystal-like coagulum, and the latex had a particle size increase up to 156 nm compared with ∼100 nm for the other chain extensions. Although low conversion was obtained, all MWDs (Fig. S2D–F) showed clear shifting from the seed latex indicating that the system was still under RAFT control. ¹H NMR of the methylated polymers (Fig. S3) revealed that for chain extension 2–4 with high *t*BA conversion, the experimental LA content followed a similar trend as for the seed latexes. The experimental LA content for chain extension 2 (5 mol% LA) was 4.7%, chain extension 3 (10 mol% LA) was 9.1% and chain extension 4 (20 mol% LA) was 19.6%. This corresponds to a similar LA conversion value around 90% as for the seed latexes. The experimental LA content was 36.7% and 43.6% for chain extension 5 and 6, respectively, highlighting that LA was being incorporated faster than *t*BA. Interestingly, LA reached full conversion for chain extension 5, even though only 82.7% BA conversion was reached. It is apparent that there is an upper limit of LA incorporation into the copolymer before colloidal instability and reduced comonomer conversion become issues.

### Degradation of PBA-*b*-P*t*BA diblock copolymers

Degradation of the diblock copolymers was explored using the DMF approach for chain extension 2–6 and the TCEP approach for chain extension 2. As with the seed latexes, using the TCEP approach for degradation of chain extension 2 resulted in only a small reduction in $M_n$ from 57 000 to 48 000 g mol⁻¹ (Fig. 5 and Table 4). In contrast, the DMF approach resulted in $M_n$ reduction to 5000 g mol⁻¹. For chain extension 3–6, the final $M_{n,exp}$ for all the degraded products ranged between 600–1000 g mol⁻¹ (Table 4). MWDs for chain extension 3–6 (Fig. 5) all show that the main peak for the degraded product is similar, the differences between the MWDs is the presence of high MW shoulders. The high MW shoulders decreased with increasing amount of LA. From the theoretical minimum $M_n$ calculations after degradation (Table S6), good agreement with the experimental $M_n$ is seen for chain extension 3–6. Chain extension 2 showed a slightly higher experimental (5000 g mol⁻¹ compared to 2700 g mol⁻¹), suggesting that extent of degradation of this system was less than 100%. The degradation studies highlight that above 10 mol% LA incorporation, the increased degradation benefits in terms of $M_n$ are minimal. It is again noted, as with the seed latex degradation, that the degraded polymer comprises components of lower MW than the original macroRAFT – this is for reasons outlined in the section above on seed latex degradation.

### Synthesis of PBA-*b*-PSt diblock copolymers

With the conditions and limitations of P(BA-*stat*-LA)-*b*-P(*t*BA-*stat*-LA) diblock copolymers established, attention shifted to a more industrially relevant system. PBA-*b*-PSt copolymers are widely employed in industrial applications as the high stiffness imparted by PSt and the elastic/adhesive properties of PBA result in a desirable polymeric material. Hawker and coworkers[24,25] have previously showed that LA can be copolymerized with St in both miniemulsion and solution polymerizations. As the previous section showed, incorporation of LA above 10 mol% has minimal increased degradation benefits, whilst resulting in lower conversions and colloidal instability. Therefore, a series of three PBA-*b*-PSt diblock copolymers were designed with 0, 5 and 10 mol% LA, respectively (Table S4). The first step was the synthesis of P(BA-*stat*-LA) seed latexes

**Table 3** Experimental conditions and results for synthesis of P(BA-*stat*-LA)-*b*-P(*t*BA-*stat*-LA) diblock copolymers using P(BA-*stat*-LA) seed latexes (seed latex 1–6, Table S2) (see Table S3 for further details)

| Chain extension | Mol%$_{LA,th}$ | DP | [RAFT]/[I] | SC (%) | $X^a$ *t*BA (%)/*t* (h) | $M_{n,theo}$[b] | $M_{n,exp}$[c]/Đ | $Z_{av}$ (nm)/PDI[d] | Mol%$_{LA,exp}$ | $X^f$ LA (%) |
|---|---|---|---|---|---|---|---|---|---|---|
| 1 | 0 | 400 | 10.0 | 20.1 | 100/3 | 77 250 | 66 650/2.08 | 99/0.05 | 0 | — |
| 2 | 5 | 399 | 10.1 | 20.3 | 100/6 | 79 400 | 57 100/2.00 | 102/0.05 | 4.7 | 94 |
| 3 | 10 | 400 | 10.5 | 20.0 | 99.0/6 | 81 950 | 43 650/1.93 | 103/0.10 | 9.1 | 89 |
| 4 | 20 | 401 | 10.3 | 20.0 | 95.0/6 | 86 700 | 58 300/2.35 | 85/0.05 | 19.6 | 94 |
| 5 | 30 | 401 | 10.1 | 20.1 | 82.7/6 | 91 400 | 43 700/2.05 | 114/0.10 | 36.7 | 100 |
| 6 | 40 | 402 | 10.0 | 20.1 | 40.0/6 | 96 200 | 35 300/1.94 | 156/0.10$^e$ | 43.6 | 70 |

$^a$ Conversion/time determined by ¹H NMR. $^b$ Theoretical $M_n$ calculated from eqn (S1). $^c$ $M_n$ and Đ determined by SEC in THF calibrated with PS standards. $^d$ Z-Average diameter and PDI by DLS. $^e$ DLS performed on latex without coagulum. $^f$ Conversion calculated from $X$ BA, $X$ *t*BA and experimental mol% LA.
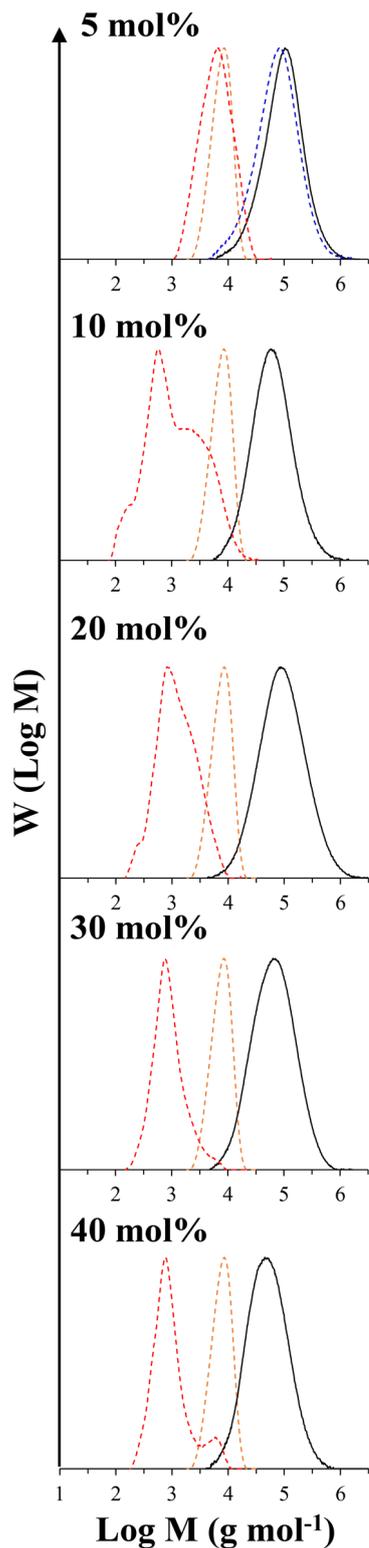
**Fig. 5** MWDs for P(BA-*stat*-LA)-*b*-P(*t*BA-*stat*-LA) diblock copolymers (chain extension 2–6, Table 3) before (black trace) and after degradation *via* both TCEP degradation approach (blue dotted trace) and DMF degradation approach (red dotted trace) with macroRAFT (orange dotted trace) for visual guide.

using the same conditions as for the seed latex synthesis above except for an increase in SC from 20% to 30%. All seed latexes reached high conversion within 6 h with $M_{n,exp} \approx M_{n,th}$ (Table S4). The MWDs (Fig. 6) were all monomodal with Đ decreasing from ~1.7 for seed latex 1–6 (Table 1) to ~1.2–1.3 (Table S4). The particle size of the seed latexes increased from ~78 nm to 90 nm with the increased SC.

The seed latexes were all chain extended to synthesize P(BA-*stat*-LA)-*b*-P(St-*stat*-LA) diblock copolymers with 0, 5 and 10 mol% LA in each of the blocks (Table S4) targeting a DP of 200 for the P(St-*stat*-LA) block. This was selected such that the PBA-*b*-PSt diblock (0 mol% LA) would result in a theoretical $T_g$ of 10 °C (according to the Fox equation) for the random copolymer equivalent. As a result, combined with the outer layer of the particles being the PBA block, it would be expected that these diblock copolymers can undergo film formation directly from the aqueous latex at room temperature. As PSt is a high $T_g$ polymer and previous works showing the increased control from hydrophobic initiators,[58,59] the reaction temperature was increased to 80 °C and AIBN was used as the initiator at a [RAFT]/[I] ratio of ~10 with SC = 20%. PBA-*b*-PSt diblock (0 mol% LA) reached 97.5% conversion in 6 h with a $M_{n,exp}$ slightly higher than $M_{n,th}$ (Table S4). The LA conversion was 91%, similar to results above. The MWD (Fig. 6A) was monomodal with a final Đ of 1.26. The PBA-*b*-PSt diblock (5 mol% LA) reached 98.1% conversion in 8 h and as with the PBA-*b*-PSt diblock (0 mol% LA) had a $M_{n,exp}$ slightly higher than $M_{n,th}$ (Table S4). The MWD (Fig. 6B) was monomodal with a final Đ of 1.25. For PBA-*b*-PSt diblock (10 mol% LA), only 78.5% conversion was reached after 8 h. Interestingly, the LA conversion was 100%. After 8 h, less than 1% of the initial AIBN remains,[46] so full conversion is unlikely to be reached. The MWD (Fig. 6C) was still monomodal with a final Đ of 1.29. All three diblocks had similar particle sizes ranging from 101 nm to 106 nm with low PDI < 0.06. ^{1}H NMR of the methylated polymers (5 and 10 mol% LA) showed incorporation of 4.6 and 11.7% LA (Fig. S4). The slightly higher than theoretical incorporation in the PBA-*b*-PSt diblock with 10 mol% LA can be attributed to the lower conversion of St. DSC measurements were performed on latexes freeze dried for 24 h, revealing two distinct $T_g$ values for each diblock copolymer (Fig. S5 and Table S7), the low temperature $T_g$ value corresponding to the PBA block and the high $T_g$ value for the PSt block. The effect of LA on $T_g$ is the low $T_g$ value shifting to a higher temperature from −43 °C for 0 mol% LA to −35.8 °C for 10 mol% LA, whereas the high $T_g$ value decreased from 102.8 °C for 0 mol% LA to 77.5 °C for 10 mol% LA. Although LA impacts both $T_g$ values, the overall impact on physical properties would be expected to be minimal. Interestingly, the results suggest that the incorporation of LA into a fully random PBA-PS copolymer would result in no significant effect on the overall $T_g$.

The PBA-*b*-PSt diblocks were cast directly from the latex at room temperature and allowed to dry for 7 days (Fig. S6). All three diblocks were able to film form at room temperature. The PBA-*b*-PSt diblocks (0 and 5 mol% LA) showed minor cracking around the edges and on the surface. To explore the

**Table 4** $M_{n,exp}$ and $Đ$ for chain extension 2–6 (Table 3) before degradation and after degradation *via* the TCEP degradation approach and the DMF degradation approach

| Chain extension | 2 | 3 | 4 | 5 | 6 |
|---|---|---|---|---|---|
| Mol%$_{LA,th}$ | 5 | 10 | 20 | 30 | 40 |
| $M_{n,exp}$ (g mol$^{-1}$)/$Đ^a$ | | | | | |
| Seed latex | 57 100/2.00 | 43 650/1.93 | 58 300/2.35 | 43 700/2.05 | 35 300/1.94 |
| TCEP degradation | 48 000/2.13 | — | — | — | — |
| DMF degradation | 5000/1.48 | 670/3.38 | 920/1.83 | 750/1.56 | 770/1.84 |

$^a$ $M_n$ and $Đ$ determined by SEC in THF calibrated with PS standards.
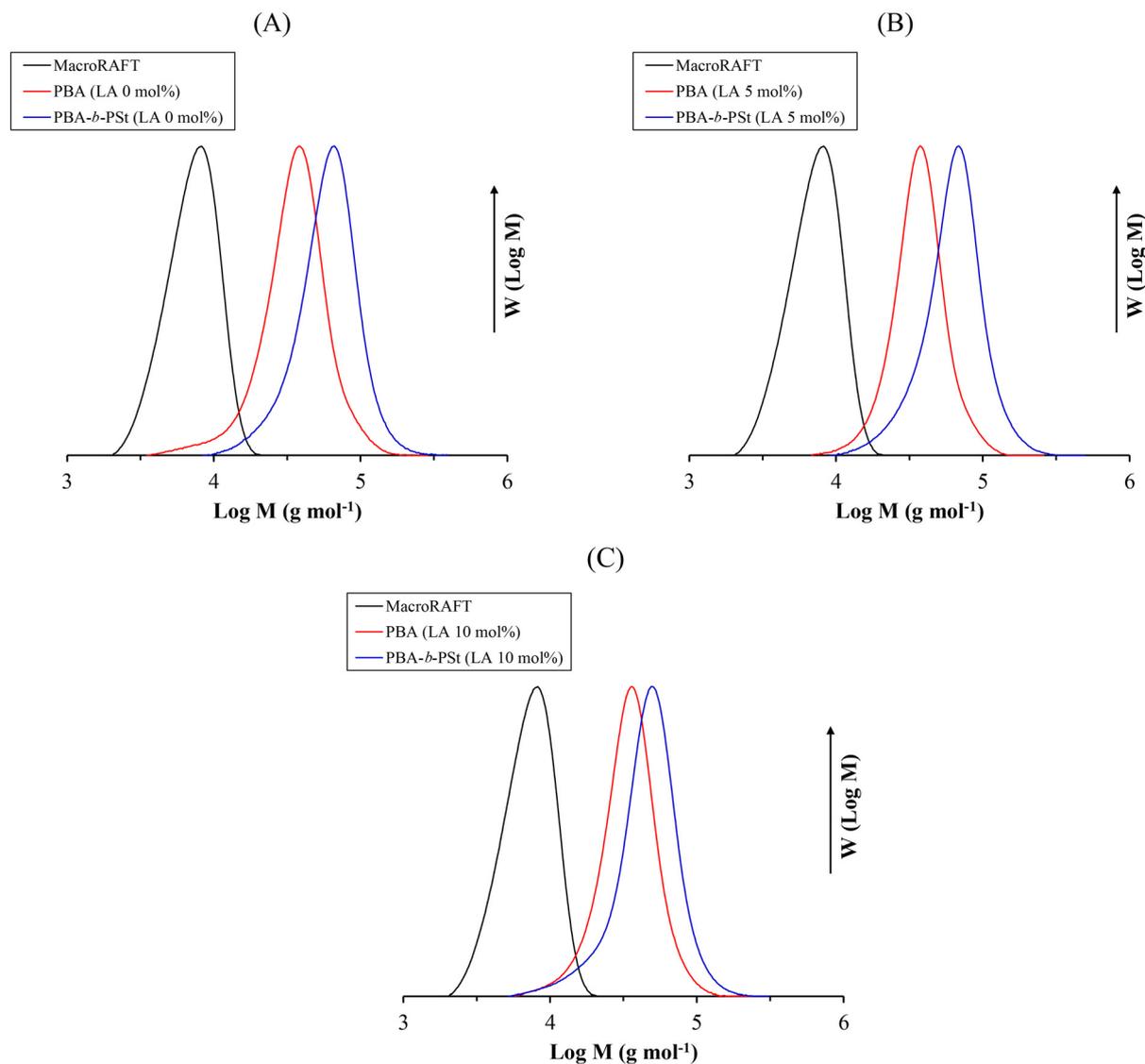


**Fig. 6** MWDs for P(BA-*stat*-LA)-*b*-P(St-*stat*-LA) diblock copolymers (Table S4) chain extended from P(BA-*stat*-LA) seed latexes: (A) PBA-*b*-PSt diblock (0 mol% LA), (B) PBA-*b*-PS diblock (5 mol% LA), and (C) PBA-*b*-PSt diblock (10 mol% LA).

effect of LA on the mechanical properties, uniaxial tensile testing was performed. The tensile strength (maximum stress at break; $\sigma_{max}$), strain at break ($\varepsilon_f$), and Young's modulus ($E$) are listed in Table S8. The difference between PBA-*b*-PSt diblock (0 mol% LA) and PBA-*b*-PS diblock (5 mol% LA) are minimal with a small decrease in both tensile strength (22.0 ± 1.3 to 20.4 ± 1.1 MPa) (Fig. 7A) and strain at break (130 ± 10 to 106 ± 3%) (Fig. 7B), but an increase in Young's modulus (36.0
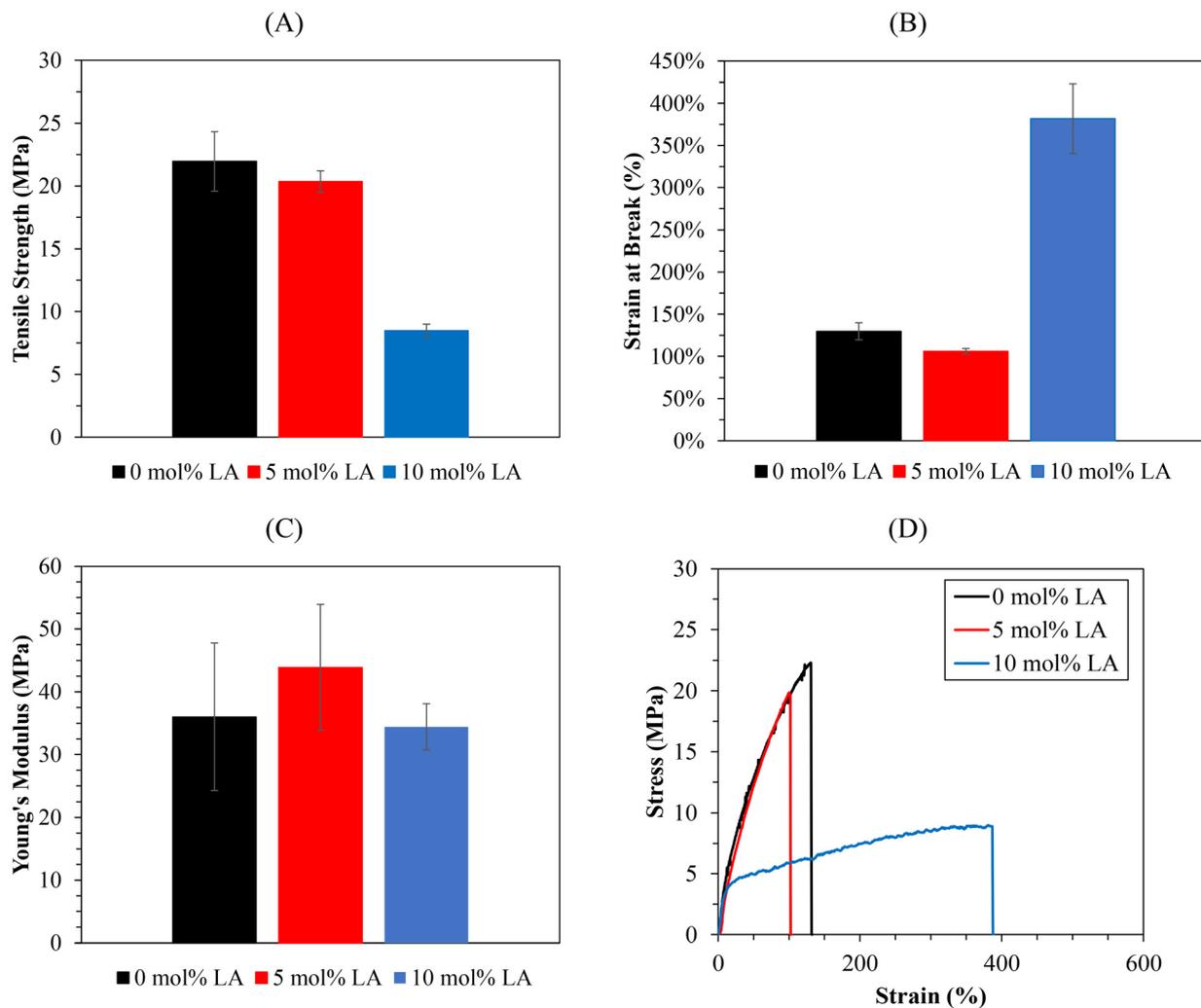
**Fig. 7** Uniaxial tensile testing results of P(BA-*stat*-LA)-*b*-P(St-*stat*-LA) diblock copolymers (Table S4) cast directly from latex: average (A) tensile strength (MPa), (B) strain at break (%), and (C) Young's modulus (MPa) and (D) representative stress strain curves.

± 11.7 to 43.9 ± 10.0 MPa) (Fig. 7C) on incorporation of LA. The representative stress–strain curves (Fig. 7D) show almost identical deformation behaviour. These results indicate that the incorporation of 5 mol% LA only has minimal impacts on the mechanical properties. In contrast PBA-*b*-PSt diblock (10 mol% LA) does exhibit different mechanical properties with lower tensile strength (8.5 ± 0.5 MPa) but increased strain at break (382 ± 41%). The Young's modulus, however, is very similar to the other two diblocks. The difference in mechanical properties can be mainly attributed to the lower St content in the second block in this case rather than the impact of LA incorporation.[50,60]

The degradation of the PBA-*b*-PSt diblocks directly from the latex and the dried film were subsequently tested. All degradations were performed at 100 °C in 5 ml of DMF open to air for 18 h. The latex degradations were performed using the same concentrations as for previous degradations. The films were dissolved in DMF at three different concentrations to explore the effect of concentration. The lowest concentration

of 40 mg in 5 ml DMF corresponds to the polymer content of the latex degradations. Medium and high concentration were 80 mg and 400 mg of films, respectively. The dried film of PBA-*b*-PSt diblock (0 mol% LA) was tested at low concentration to see if any changes occurred without LA. From the $M_{n,exp}$ a small reduction in MW was seen (Table 5), however, examination of the MWD (Fig. 8A) reveals that the two peaks are almost identical. This shows that negligible degradation of PBA-*b*-PSt diblock (0 mol% LA) takes place as anticipated. The PBA-*b*-PSt diblock (5 mol% LA) showed a large reduction in MW in all cases (latex and films) (Table 5). The degradation of the latex resulted in the largest reduction in MW from 55 500 to 3700 g mol$^{-1}$. All three films also resulted in large degradation with no significant effect of concentration. The MWDs (Fig. 8B) show that the peaks for all four degradations are very similar. In contrast, the degradation of the PBA-*b*-PSt diblock (10 mol% LA) was affected by the concentration. The degradation directly from latex and the low concentration film resulted in a reduction from 39 450 to 2100 g mol$^{-1}$ and

**Table 5** $M_{n,exp}$ and Đ for P(BA-*stat*-LA)-*b*-P(St-*stat*-LA) diblock copolymers (Table S4) before degradation and after degradation of latex and dried films *via* DMF degradation approach at low, medium and high concentration

| PBA-*b*-PSt diblock | 0 mol% LA | 5 mol% LA | 10 mol% LA |
|---|---|---|---|
| Mol%$_{LA,th}$ | 0 | 5 | 10 |
| Mol%$_{LA,exp}$ | 0 | 4.6 | 11.7 |
| $M_{n,exp}$ (g mol$^{-1}$)/Đ$^a$ | | | |
| Diblock | 52 450/1.26 | 55 500/1.25 | 39 450/1.29 |
| Latex | — | 3700/2.03 | 2100/2.06 |
| Film low concentration | 48 700/1.28 | 5950/1.60 | 2200/1.90 |
| Film medium concentration | — | 5650/1.63 | 4350/1.19 |
| Film high concentration | — | 4400/1.42 | 21 400/1.65 |

$^a$ $M_n$ and Đ determined by SEC in THF calibrated with PS standards.

2200 g mol$^{-1}$, respectively. The medium film concentration had a reduction to 4350 g mol$^{-1}$ and the high concentration film only reduced to 21 400 g mol$^{-1}$ (Table 5). Note that even for the highest film concentration, complete dissolution of the film was observed. Comparing the MWDs for the degradations (Fig. 8C), the main peak of latex, film low and medium concentration align, however, the MWD for the latex (red dotted line) and film low concentration (green dotted line) have low MW shoulders which result in the $M_{n,exp}$ being lower than for medium concentration. These results suggest that the effect of concentration difference between low and medium concentration is minimal. The reasons for the high concentration film not degrading as much as the other films are unclear. One potential cause is that the dissolved oxygen was lower in
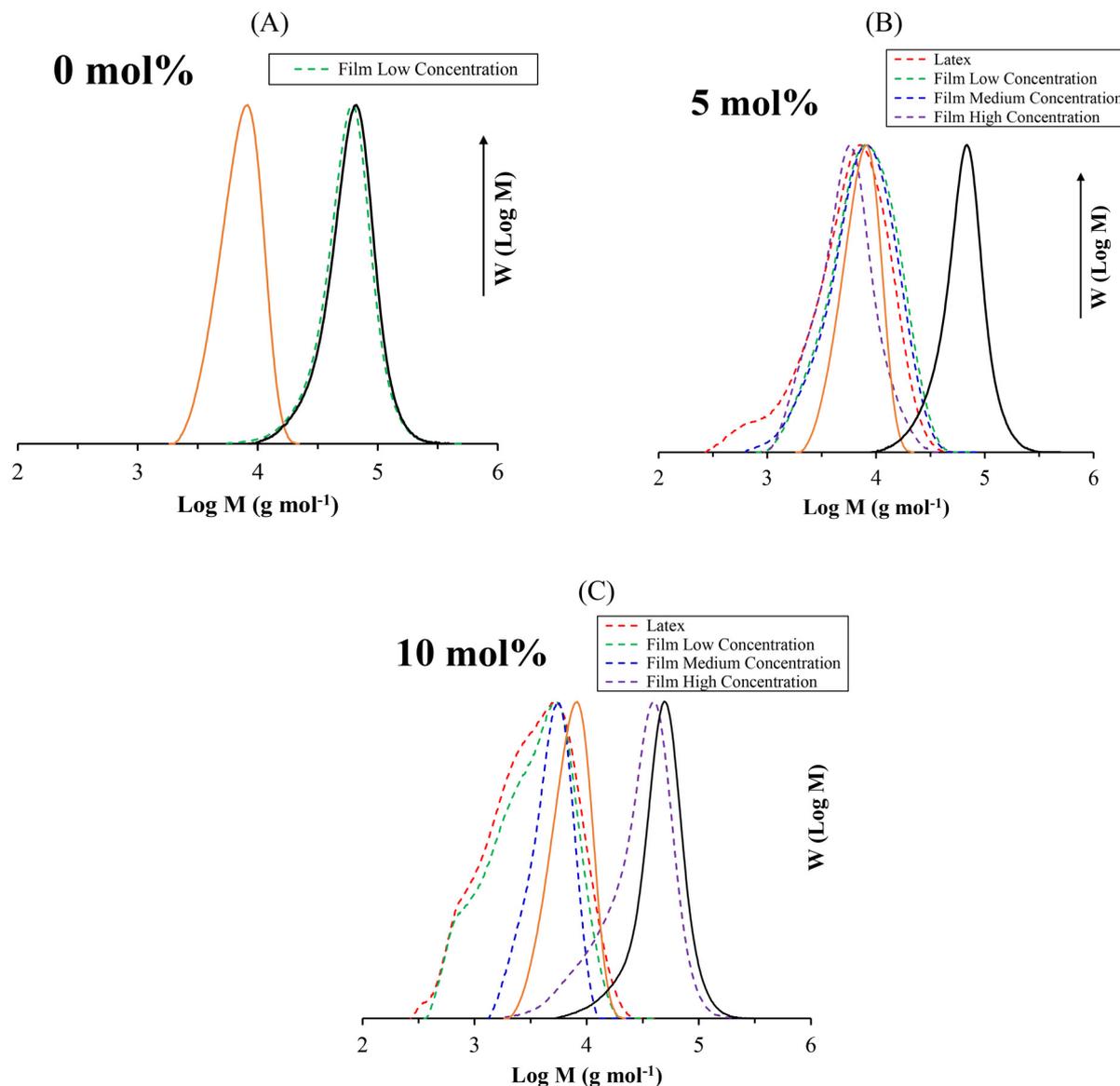


**Fig. 8** MWDs for P(BA-*stat*-LA)-*b*-P(St-*stat*-LA) diblock copolymers (Table S4) before degradation (black trace) and after degradation of latex and dried films *via* DMF degradation approach at low, medium and high concentration with macroRAFT (orange trace) for visual reference: (A) PBA-*b*-PSt diblock (0 mol% LA), (B) PBA-*b*-PSt diblock (5 mol% LA), and (C) PBA-*b*-PSt diblock (10 mol% LA).

solution. Okayama et al.[24] showed the oxygen presence is vital for degradation and a lower dissolved oxygen content may have resulted in incomplete or no degradation. The experimental $M_n$ values were slightly higher than the minimum theoretical values (Table S9) corresponding to the maximum level of degradation (as explained above) for both 5 and 10 mol% LA. Seed latex 2 and 3 (Table 1), showed good agreement with the theoretical minimum $M_n$ for the PBA seed latexes with 5 and 10 mol% LA, respectively, suggesting that the extent of degradation of the PSt block is the likely cause of the difference observed.

Overall, the degradation of PBA-b-PSt diblock (5 mol% LA) films has shown that degradable polymer films can be synthesized with only minimal change in mechanical properties. This highlights the potential practicability for these systems to be used in industrial applications.

## Conclusions

This study demonstrates the use of macroRAFT-mediated emulsion polymerization to synthesize PBA seed latexes with up to 40 mol% LA incorporation. These can be successfully degraded to low molecular weight components (<1000 g mol$^{-1}$) using thermolysis in DMF. Chain extension with tBA and LA further enabled the formation of diblock copolymers, with degradation testing showing that 5–10 mol% LA incorporation offers an appropriate balance between degradability and synthesis challenges that arise for higher mol% LA. Industrially relevant PBA-b-PSt diblock copolymers with 5 and 10 mol% LA were synthesized successfully and were shown to be able to film form directly from the latex at room temperature. Notably, PBA-b-PSt (5 mol% LA) exhibited minimal changes in mechanical properties while maintaining significant degradability, underscoring their potential for industrial applications where environmental sustainability and material performance are both critical. It is worth mentioning that DMF is not classified as a green solvent, and future alternatives that are more environmentally friendly may be cyrene and 1-butylpyrrolidin-2-one. Moreover, in an industrial process, the possibility of solvent recycling should also be considered. Overall, these findings pave the way for scalable, environmentally friendly production of degradable polymeric materials suitable for many industrial applications.

## Conflicts of interest

There are no conflicts to declare.

## Data availability

All relevant data supporting the findings of this study are available from the corresponding author upon reasonable request.

Supplementary information (SI) is available. See DOI: https://doi.org/10.1039/d5gc04609b.

## References

1 A. Kumar, V. K. Thakur, H. Y. Nezhad and K.-S. Lee, Sci. Rep., 2024, 14, 9430.
2 C. Lefay and Y. Guillaneuf, Prog. Polym. Sci., 2023, 147, 101764.
3 T. Pesenti and J. Nicolas, ACS Macro Lett., 2020, 9, 1812–1835.
4 A. Tardy, J. Nicolas, D. Gigmes, C. Lefay and Y. Guillaneuf, Chem. Rev., 2017, 117, 1319–1406.
5 R. Kamiki, T. Kubo and K. Satoh, Macromol. Rapid Commun., 2023, 44, 2200537.
6 Y. Du, Y. Du, S. Lazzari, T. Reimers, R. Konradi, T. W. Holcombe and E. B. Coughlin, Polym. Chem., 2022, 13, 5829–5840.
7 A. Tardy, J.-C. Honoré, J. Tran, D. Siri, V. Delplace, I. Bataille, D. Letourneur, J. Perrier, C. Nicoletti, M. Maresca, C. Lefay, D. Gigmes, J. Nicolas and Y. Guillaneuf, Angew. Chem., Int. Ed., 2017, 56, 16515–16520.
8 M. R. Hill, E. Guégain, J. Tran, C. A. Figg, A. C. Turner, J. Nicolas and B. S. Sumerlin, ACS Macro Lett., 2017, 6, 1071–1077.
9 W. Wang, B. Rondon, Z. Wang, J. Wang and J. Niu, Macromolecules, 2023, 56, 2052–2061.
10 J. M. J. Paulusse, R. J. Amir, R. A. Evans and C. J. Hawker, J. Am. Chem. Soc., 2009, 131, 9805–9812.
11 R. A. Evans, G. Moad, E. Rizzardo and S. H. Thang, Macromolecules, 1994, 27, 7935–7937.
12 N. M. Bingham and P. J. Roth, Chem. Commun., 2019, 55, 55–58.
13 N. Gil, B. Caron, D. Siri, J. Roche, S. Hadiouch, D. Khedaioui, S. Ranque, C. Cassagne, D. Montarnal, D. Gigmes, C. Lefay and Y. Guillaneuf, Macromolecules, 2022, 55, 6680–6694.
14 M. P. Spick, N. M. Bingham, Y. Li, J. de Jesus, C. Costa, M. J. Bailey and P. J. Roth, Macromolecules, 2020, 53, 539–547.
15 M. Pięta, V. B. Purohit, J. Pietrasik and C. M. Plummer, Polym. Chem., 2023, 14, 7–31.
16 K. R. Albanese, J. Read de Alaniz, C. J. Hawker and C. M. Bates, Polymer, 2024, 304, 127167.
17 M. Raeisi and N. V. Tsarevsky, J. Polym. Sci., 2021, 59, 675–684.
18 X. Zhang and R. M. Waymouth, J. Am. Chem. Soc., 2017, 139, 3822–3833.
19 H.-T. Zhang, L.-K. Hou, G.-W. Chu, J.-X. Wang, L.-L. Zhang and J.-F. Chen, Chem. Eng. J., 2024, 482, 148816.

20  S. Han, V. A. Bobrin, M. Michelas, C. J. Hawker and C. Boyer, *ACS Macro Lett.*, 2024, **13**, 1495–1502.

21  T. O. Machado, C. J. Stubbs, V. Chiaradia, M. A. Alraddadi, A. Brandolese, J. C. Worch and A. P. Dove, *Nature*, 2024, **629**, 1069–1074.

22  F. Dawson, G. Irvine and M. Kopeć, *Polym. Chem.*, 2025, **16**, 2659–2669.

23  K. R. Albanese, P. T. Morris, J. Read de Alaniz, C. M. Bates and C. J. Hawker, *J. Am. Chem. Soc.*, 2023, **145**, 22728–22734.

24  Y. Okayama, P. Morris, K. Albanese, S. Olsen, A. Mori, J. R. de Alaniz, C. M. Bates and C. J. Hawker, *J. Polym. Sci.*, 2025, **63**, 1345–1351.

25  P. T. Morris, K. Watanabe, K. R. Albanese, G. T. Kent, R. Gupta, M. Gerst, J. Read de Alaniz, C. J. Hawker and C. M. Bates, *J. Am. Chem. Soc.*, 2024, **146**, 30662–30667.

26  K.-D. Hungenberg and E. Jahns, *Adv. Polym. Sci.*, 2018, **280**, 195–214.

27  P. A. Lovell and F. J. Schork, *Biomacromolecules*, 2020, **21**, 4396–4441.

28  M. Aguirre, N. Ballard, E. Gonzalez, S. Hamzehlou, H. Sardon, M. Calderon, M. Paulis, R. Tomovska, D. Dupin, R. H. Bean, T. E. Long, J. R. Leiza and J. M. Asua, *Macromolecules*, 2023, **56**, 2579–2607.

29  F. D'Agosto, J. Rieger and M. Lansalot, *Angew. Chem., Int. Ed.*, 2020, **59**, 8368–8392.

30  N. J. W. Penfold, J. Yeow, C. Boyer and S. P. Armes, *ACS Macro Lett.*, 2019, **8**, 1029–1054.

31  F. Ishizuka, H. J. Kim, R. P. Kuchel, Y. Yao, S. Chatani, H. Niino and P. B. Zetterlund, *Eur. Polym. J.*, 2022, **169**, 111134.

32  H. J. Kim, F. Ishizuka, R. P. Kuchel, S. Chatani, H. Niino and P. B. Zetterlund, *Polym. Chem.*, 2022, **13**, 1719–1730.

33  S. W. Thompson, T. R. Guimarães and P. B. Zetterlund, *Polym. Chem.*, 2022, **13**, 5048–5057.

34  A. A. Cockram, R. D. Bradley, S. A. Lynch, P. C. D. Fleming, N. S. J. Williams, M. W. Murray, S. N. Emmett and S. P. Armes, *React. Chem. Eng.*, 2018, **3**, 645–657.

35  C. J. Ferguson, R. J. Hughes, D. Nguyen, B. T. T. Pham, R. G. Gilbert, A. K. Serelis, C. H. Such and B. S. Hawkett, *Macromolecules*, 2005, **38**, 2191–2204.

36  C. J. Ferguson, R. J. Hughes, B. T. T. Pham, B. S. Hawkett, R. G. Gilbert, A. K. Serelis and C. H. Such, *Macromolecules*, 2002, **35**, 9243–9245.

37  S. Zhang, R. Li and Z. An, *Angew. Chem., Int. Ed.*, 2024, **63**, e202315849.

38  P. Galanopoulo, N. Gil, D. Gigmes, C. Lefay, Y. Guillaneuf, M. Lages, J. Nicolas, F. D'Agosto and M. Lansalot, *Angew. Chem., Int. Ed.*, 2023, **62**, e202302093.

39  M. Lages, N. Gil, P. Galanopoulo, J. Mougin, C. Lefay, Y. Guillaneuf, M. Lansalot, F. D'Agosto and J. Nicolas, *Macromolecules*, 2022, **55**, 9790–9801.

40  P. Galanopoulo, N. Gil, D. Gigmes, C. Lefay, Y. Guillaneuf, M. Lages, J. Nicolas, M. Lansalot and F. D'Agosto, *Angew. Chem., Int. Ed.*, 2022, **61**, e202117498.

41  J. Li, H. Yang, Q. Jiang, J. Li, B. Jiang, X. Xue, S. Komarneni and W. Huang, *Chem. Commun.*, 2025, **61**, 3692–3695.

42  J. Fang, S. Wang and Y. Luo, *AIChE J.*, 2020, **66**, e16781.

43  J. Fang, X. Gao and Y. Luo, *Polymer*, 2020, **201**, 122602.

44  T. R. Guimarães, M. Khan, R. P. Kuchel, I. C. Morrow, H. Minami, G. Moad, S. b. Perrier and P. B. Zetterlund, *Macromolecules*, 2019, **52**, 2965–2974.

45  H. J. Kim, F. Ishizuka, R. P. Kuchel, Y. Yao, S. Chatani, H. Niino and P. B. Zetterlund, *Eur. Polym. J.*, 2023, **193**, 112118.

46  S. W. Thompson, T. R. Guimarães and P. B. Zetterlund, *Macromolecules*, 2023, **56**, 9711–9724.

47  M. Khan, T. R. Guimarães, R. P. Kuchel, G. Moad, S. Perrier and P. B. Zetterlund, *Angew. Chem., Int. Ed.*, 2021, **60**, 23281–23288.

48  M. Khan, T. R. Guimaraes, K. Choong, G. Moad, S. Perrier and P. B. Zetterlund, *Macromolecules*, 2021, **54**, 736–746.

49  G. K. K. Clothier, T. R. Guimarães, M. Khan, G. Moad, S. Perrier and P. B. Zetterlund, *ACS Macro Lett.*, 2019, **8**, 989–995.

50  S. W. Thompson, J. Li, D. Singh, G. J. Sanjayan and P. B. Zetterlund, *ACS Appl. Polym. Mater.*, 2024, **6**, 6495–6507.

51  S. W. Thompson, T. R. Guimarães and P. B. Zetterlund, *Biomacromolecules*, 2020, **21**, 4577–4590.

52  G. K. K. Clothier, T. R. Guimarães, L. T. Strover, P. B. Zetterlund and G. Moad, *ACS Macro Lett.*, 2023, **12**, 331–337.

53  G. K. K. Clothier, T. R. Guimarães, S. W. Thompson, J. Y. Rho, S. Perrier, G. Moad and P. B. Zetterlund, *Chem. Soc. Rev.*, 2023, **52**, 3438–3469.

54  H. Takahashi, Y. Bungo and K. Mikuni, *Biosci., Biotechnol., Biochem.*, 2011, **75**, 633–637.

55  Z. Shaked, R. P. Szajewski and G. M. Whitesides, *Biochemistry*, 1980, **19**, 4156–4166.

56  G. Eda, J. Liu and S. Shivkumar, *Eur. Polym. J.*, 2007, **43**, 1154–1167.

57  T. Gruendling, T. Junkers, M. Guilhaus and C. Barner-Kowollik, *Macromol. Chem. Phys.*, 2010, **211**, 520–528.

58  G. K. K. Clothier, T. R. Guimarães, G. Moad and P. B. Zetterlund, *Macromolecules*, 2022, **55**, 1981–1991.

59  G. K. K. Clothier, T. R. Guimarães, G. Moad and P. B. Zetterlund, *Macromolecules*, 2021, **54**, 3647–3658.

60  A. Pérez, E. Kynaston, C. Lindsay and N. Ballard, *Prog. Org. Coat.*, 2022, **168**, 106882.